Dust records from three ice cores: Relationships to spring atmospheric circulation over the Northern Hemisphere

Article *in* Atmospheric Environment · November 2003

DOI: 10.1016/j.atmosenv.2003.08.010

Shichang Kang
State Key Laboratory of Cryosphere Sciences, Chinese Academy of Scienc…

Yuping Yan
Wuhan University

Jiawen Ren
Chinese Academy of Sciences

Atmospheric Environment 37 (2003) 4823–4835

ATMOSPHERIC ENVIRONMENT

www.elsevier.com/locate/atmosenv

Dust records from three ice cores: relationships to spring atmospheric circulation over the Northern Hemisphere

Shichang Kang[a,b,*], Paul A. Mayewski[a,c], Yuping Yan[a], Dahe Qin[b], Tandong Yao[b,d], Jiawen Ren[b]

[a] *Climate Change Institute, University of Maine, 303 Bryand Hall, Orono, ME 04469, USA*

[b] *Key Laboratory of Ice Core and Cold Regions Environment, Cold and Arid Environmental and Engineering Research Institute, Chinese Academy of Sciences, Lanzhou 730000, China*

[c] *Department of Earth and Environmental Sciences, University of Maine, Orono, ME 04469, USA*

[d] *Institute of Tibetan Plateau, Chinese Academy of Sciences, Beijing, China*

Received 10 February 2003; accepted 1 August 2003

Abstract

Non-sea-salt Mg^{2+} ($nssMg^{2+}$) records from three Northern Hemisphere ice cores (Mt. Everest, Himalayas; Mt. Logan, Yukon Territory; and 20D, southern Greenland) are presented as a proxy of atmospheric dust. $NssMg^{2+}$ concentrations of both Mt. Everest and 20D ice core have increased since the 20th century. Relationships between the three ice core annual $nssMg^{2+}$ series and instrumental sea-level pressure (SLP) series of spring (March–April–May) are investigated for the last century (AD 1899–1996), in order to develop an understanding of dust aerosol transport over the Northern Hemisphere during the spring season. On a hemispheric scale, an enhanced spring Arctic High weakens dust aerosol transport from central Asia to subarctic regions (e.g., southern Greenland and Yukon Territory), but strengthens transport of dust to the Himalaya (e.g., Mt. Everest). An intensification of the Siberian High may strengthen transport of dust aerosols to Greenland, and an enhancement of the Tibetan High strengthens transport to Himalaya and Yukon regions in spring. A stronger spring Azores High favors dust transport to both the Himalayas and south Greenland. On a regional scale, a deepened spring Icelandic Low and Aleutian Low increases transport of dust aerosols to Greenland and the Yukon Territory, respectively. Understanding these transport patterns is significant for the interpretation of ice core records and reconstruction of atmospheric circulation using longer records.

Keywords: $NssMg^{2+}$ records; Ice core; Dust aerosols; Sea-level pressure; Northern Hemisphere

1. Introduction

Atmospheric dust over the Northern Hemisphere is mainly imported by dust storms (about 10^6–$10^7\,t\,yr^{-1}$) (Iwasaka et al., 1983) and the arid and semi-arid regions of central Asia are a major source area for dust aerosols to the Northern Hemisphere (Parrington et al., 1983; Gao et al., 1992; Husar et al., 2001). Dust storms can be major calamities and the range covered by dust storms can reach 10^6–$10^7\,km^2$ (Iwasaka et al., 1983). The peak in dust storm activity throughout central Asia occurs from mid-February to late May, with a strong maximum in late April–early May (Merrill et al., 1989). Studies based on satellite and ground-based observations and modeling show that dust aerosols have a large impact on the climate system (Li et al., 1996; Moulin et al., 1997; Takemura et al., 2000; Sassen, 2002). Dust aerosols scatter the solar radiation back to space and absorb the ultraviolet radiation. In addition, aridification and dust storms are hazards to agriculture and ecosystem health. High-resolution ice core records provide a convenient

*Corresponding author. Climate Change Institute, University of Maine, 303 Bryand Hall, Orono, ME 04469, USA. Tel.: +1-207-581-2840; fax: +1-207-581-1203.

E-mail address: shichang.kang@maine.edu (S. Kang).

1352-2310/$ - see front matter © 2003 Elsevier Ltd. All rights reserved.
doi:10.1016/j.atmosenv.2003.08.010

means to measure the depositional flux of atmospheric dust and the history of these storms.

Relationships developed between glaciochemical records from bipolar and Asia and atmospheric circulation demonstrate that ice core records provide a proxy for the reconstruction of atmospheric circulation (Kreutz et al., 2000; Meeker and Mayewski, 2002; Kang et al., 2002a). The methodology employed in the reconstructions can also be used to determine the spatial and temporal controls on glaciochemical records (such as dust transport pathway and strength). In order to explore these processes, this paper is focused on the comparison between ice core chemical records from three Northern Hemisphere (Mt. Everest, southern Tibetan Plateau; 20D, southern Greenland; and Mt. Logan, Yukon Territory) and instrumental sea-level pressure (SLP) series, allowing investigation of the atmospheric transport patterns of dust aerosols, particularly during the spring dust storm season.

2. Atmospheric circulation and climate over the ice core sites

2.1. Mt. Everest, southern Tibetan Plateau

The southeast portion of the Asia continent is mainly influenced by polar air masses originating in the Arctic, continental air masses originating over central Asia, and equatorial-maritime air masses originating in the Pacific and Indian Oceans (Bryson, 1986). The Tibetan Plateau plays a central role in climatology of the region. It blocks mid-latitude westerlies and splits the jet into two currents that flew south and north of the plateau. A complete reversal of weather patterns occurs from summer to winter. In summer, low-pressure over the plateau induces a supply of moist and warm air from the Indian and Pacific Oceans to the continent (summer monsoon). In winter, high-pressure drives cold and dry air moving out of the plateau (winter monsoon) (Bryson, 1986; Tang, 1998). The transition in atmospheric circulation takes place in spring and autumn. In the earlier spring, the westerlies begin their seasonal migration northwards. At this time the northerly jet strengthens and begins to extend across central China and into Japan, and the southerly branch remains south of Tibet, weakening in intensity. In late spring, the southern branch of the jet breaks down, becoming intermittent, gradually shifting northwards over the Tibetan Plateau (Barry and Chorley, 1998).

2.2. 20D, southern Greenland ice sheet

The principal features of the mean North Atlantic pressure pattern are the Icelandic Low and the Azores High. They are present during all seasons, although their location and relative intensity change considerably. The Siberian winter anticyclone also influences the North Atlantic climate. Studies of backward air mass trajectories (Davidson et al., 1993; Kahl et al., 1997) show that Greenland is mainly influenced by air masses from the North America, the North Pacific, east Asia, west Asia/Europe, and the North Atlantic. Air masses from east Asia and the North America are dominant in winter and summer. Trajectories in spring, especially in April, suggest Eurasia (transport over the North Pole), eastern North America, and western Europe as potential air mass source regions. Air masses from the North Pacific and east Asia dominate in autumn.

2.3. Mt. Logan, Yukon Territory

For Mt. Logan (about 100 km away from the coast of the Gulf of Alaska), most of its precipitation is derived from the Gulf of Alaska. The Gulf is characterized by rapid cyclogenesis and extremely high precipitation while there is a high frequency of anticyclonic activity over the Yukon (Wilson and Overland, 1987). The meteorology of the Gulf of Alaska is influenced by the relative positions of three semi-permanent atmospheric features: the Aleutian Low, the North Pacific High and the Siberian High. The Aleutian Low occurs 25% of the time, making it the dominant influence on the coast of the Gulf of Alaska weather throughout the year (Overland and Heister, 1980). The low moves southeastward from the Bering Sea into the Gulf from August to December. In January the low-pressure center moves to the western Aleutians where it slowly weakens through July. The oceanic region is cooler than the adjacent land masses and a large high-pressure system is established over the North Pacific Ocean. It reaches maximum intensity and a northwards position in June–August and dominates almost the entire North Pacific including the Gulf of Alaska (Favorite et al., 1976). The Siberian High affects the North Pacific region from October through March. It reaches its maximum intensity in January and is associated with a huge pool of very cold winter air over eastern Asia and northern Alaska. Although rarely present in the Gulf, its sway is felt through a southward shift in the location of the Aleutian storm track and an increase in cold winds blowing from the north over the western Gulf (Wilson and Overland, 1987).

3. Methods

3.1. Coring and dating

In August 1998, an 80.4 m ice core was recovered from the East Rongbuk (ER) Glacier at an elevation of 6450 m a.s.l. on the northern slope of Mt. Everest

(27°59′N, 86°55′E) (Fig. 1). Details of the ice core site, sampling, and analysis are described by Qin et al. (2002) and Kang et al. (2002a, b). Temperature at 10 m depth at this site is $-9.6°C$ and accumulation rate is $0.4\,m\,yr^{-1}$. The ice core was sectioned at intervals between 3.5 and 5 cm (total of 1837 samples). Preservation of annual signals in the ER ice core $\delta^{18}O$ plus several chemical species (e.g., NH_4^+, Ca^{2+}, SO_4^{2-}, Mg^{2+}) series have been verified based on calibration with known bomb horizons (1954 and 1963) identified in the well-preserved total β-activity profile from this core. We counted 153 annual layers back through the entire 80.4 m ice core, indicating that our record spans the time period from AD 1845 to 1997 (at a resolution of 12 samples/year). This combination of dating techniques yields an annually resolved chronology that is accurate to within ± 1 yr at the bottom of the core.

In 1984, a 115 m ice core was drilled from site 20D (65°01′N, 44°52′W) (Fig. 1) at an elevation of 2615 m a.s.l.. The site is near the crest of the southern ice dome and is 40 km southwest of Dye 3. Accumulation rate at the site is $0.41\,m\,yr^{-1}$. The ice core was dated back to AD 1769 at the bottom of the core (at a resolution of 8 samples/year) using a variety of different seasonal indicators, historically documented volcanic events plus total β-activity signatures (Mayewski et al., 1986, 1993).

In 1980, a 103 m ice core was drilled on Mt. Logan (60°35′N, 140°30′W) (Fig. 1) in the Saint Elias Mountains, Yukon Territory, at an elevation of 5340 m a.s.l.. Temperature at 10 m depth in the firn at this site is approximately $-29°C$, suggesting very little or no summer melting. Accumulation rate at the site is $0.33\,m\,yr^{-1}$. The sectioning was designed to yield 8–12 samples/year for analysis of major ion concentration. The combination of dating techniques yield annually resolved chronologies, extending back to AD 1688 at the bottom of the Mt. Logan ice core. The detailed methods of dating were described by Holdsworth et al. (1989) and Mayewski et al. (1993).

Magnesium in an ice core has two major sources for both low-latitude and polar regions: sea-salt and crustal aerosols (Legrand and Mayewski, 1997; Kang et al., 2000). Here we use non-sea-salt Mg^{2+} ($nssMg^{2+} = Mg^{2+} - (0.12 \times Na^+)$) as a proxy for atmospheric dust aerosols. The annual $nssMg^{2+}$ concentrations of the Mt. Everest ice core (AD 1845–1997), the 20D ice core (AD 1769–1984), and the Mt. Logan ice core (AD 1750–1979) is displayed in Fig. 2. Mt. Everest $nssMg^{2+}$ concentrations are higher than those of 20D and Mt. Logan core (Table 1) probably due to its location closed to the arid regions. There is an increase trend in Mt. Everest $nssMg^{2+}$ variations since the 20th

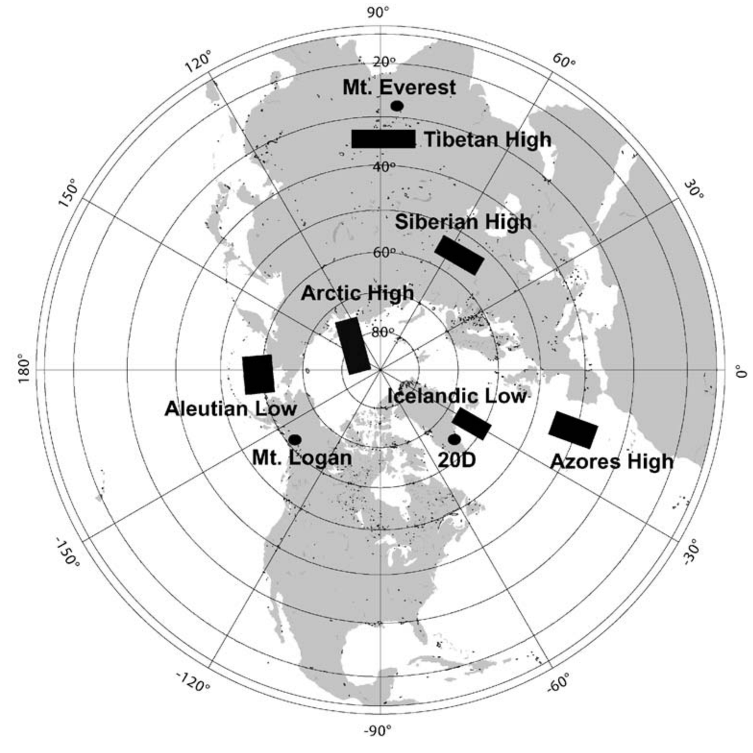

Fig. 1. Location map showing the coring sites at Mt. Everest, Mt. Logan, and 20D, as well as areas (blackened) of instrumental SLP data used for comparison with the three ice core $nssMg^{2+}$ records.

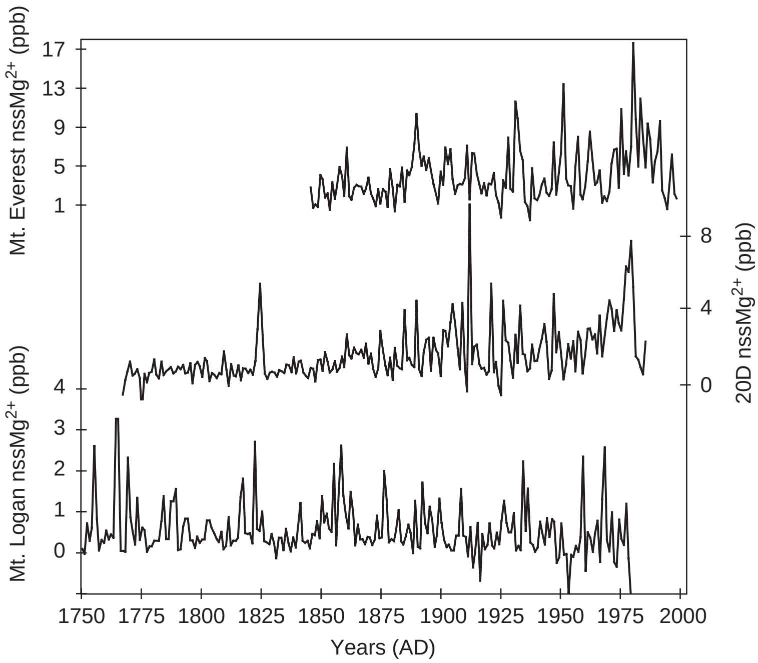

Fig. 2. Time-series of annual concentrations of $nssMg^{2+}$ from the Mt. Everest, the 20D and the Mt. Logan ice cores.

Table 1
Average concentrations ($\pm$standard deviation) of annual $nssMg^{2+}$ values from the three Northern Hemisphere ice cores (unit: ppb)

Coring sites	18th century	19th century	20th century
Mt. Everest		3.2±2.0	4.5±3.1
20D	0.5±0.6	1.1±1.0	2.3±1.8
Mt. Logan	0.7±0.8	0.6±0.5	0.4±0.6

century. The 20D $nssMg^{2+}$ concentrations have been increasing since the middle of the 19th century and a dramatic increase occurs since the 1960s. However, the slight decrease trend exists for Mt. Logan $nssMg^{2+}$ concentrations. Although the arid and semi-arid regions of central Asia are a major source area of dust aerosols for the three coring sites (Kang et al., 2002a; Kahl et al., 1997; Mckendry et al., 2001), the transport pathways of dust aerosols are diverse for the three sites. Therefore, the differences of $nssMg^{2+}$ variations between the three ice cores should be related to the long-term air pressure patterns changes and/or the changes in transport strength of dust aerosols. This will be clarified by the investigations of relationships between $nssMg^{2+}$ and SLP series.

3.2. Ice core $nssMg^{2+}$–SLP calibration

To investigate the relationship between variations of ice core $nssMg^{2+}$ concentrations and atmospheric circulation, monthly instrumental records of atmospheric SLP (1899–1996) over the Northern Hemisphere (Trenberth and Paolino, 1980; Meeker and Mayewski, 2002) were chosen to compare with the Mt. Everest, the Mt. Logan and the 20D annual $nssMg^{2+}$ series. To explore possible relationships among the annually $nssMg^{2+}$ series and monthly SLP fields, the common SLP observations are divided into three groups defined by the level of $nssMg^{2+}$ concentrations: the third lowest, the third highest, and intermediate values. Detailed methods for this analysis are described by Meeker and Mayewski (2002). Division into groups on this scale results in a conservative estimate of the SLP/ $nssMg^{2+}$ relationship(s), since only the most persistent features of the SLP fields associated with $nssMg^{2+}$ are expected to appear in the third of averages (Meeker and Mayewski, 2002). Results of this analysis reveal that $nssMg^{2+}$ display connections to spring (March–April–May: MAM) SLP over the Northern Hemisphere (Figs. 3–5).

Fig. 3 shows that Mt. Everest $nssMg^{2+}$ concentrations are related to changes in SLP of the Tibetan High over Asia. Springs in which $nssMg^{2+}$ values are lowest exhibit low-pressure anomalies in the Tibetan High (Fig. 3A). The reverse pattern is seen in Fig. 3C indicating that highest $nssMg^{2+}$ values are related to high-pressure anomalies for the Tibetan High. In addition, SLP anomalies over the Arctic, the North Pacific, and the North Atlantic are also related to high/low $nssMg^{2+}$ concentrations of the Mt. Everest ice core.

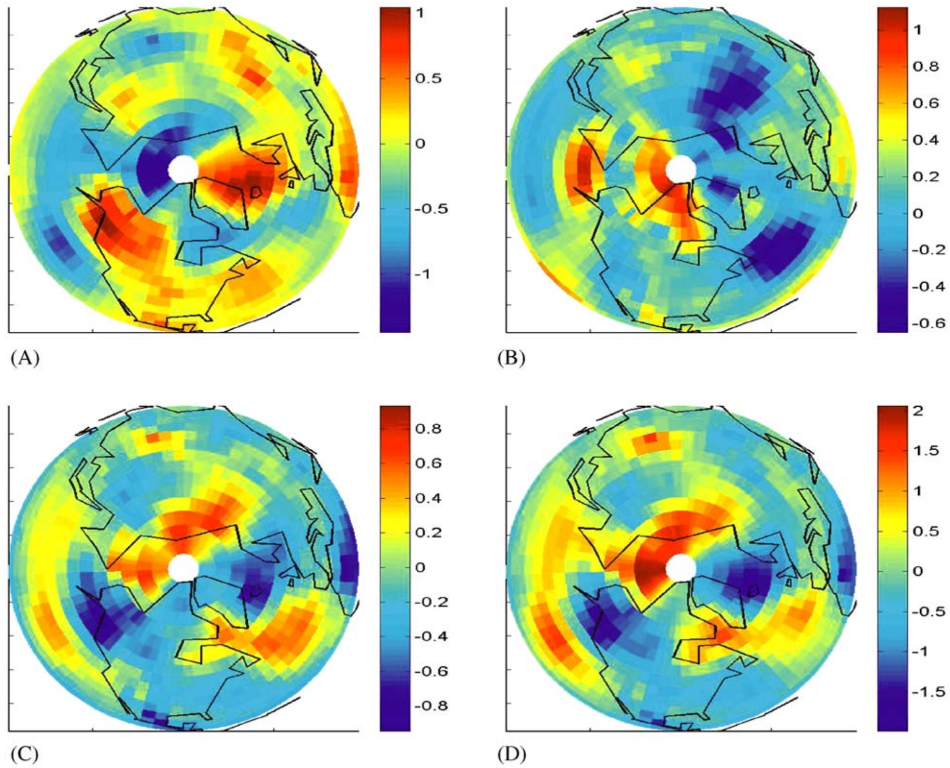

Fig. 3. Mean SLP field (all units: mb) calibrated with nssMg^{2+} concentrations from the Mt. Everest ice core: (A) mean SLP field anomaly in spring for the 33 years of lowest Mt. Everest nssMg^{2+} concentrations; (B) mean SLP field anomaly in spring for the 32 years of intermediate ones; (C) mean SLP field anomaly in spring for the 33 years of highest ones; and (D) difference SLP field in spring: mean anomaly of highest 33 years—mean anomaly of lowest 33 years.

Fig. 4 shows that nssMg^{2+} concentrations of the 20D ice core are related to SLP of the Siberian region over Eurasia. Springs in which nssMg^{2+} values are low/high (Figs. 4A and C) exhibit low/high anomalies for the Siberian SLP. Meanwhile, 20D nssMg^{2+} has a strong connection with spring SLP of the Icelandic Low and the Azores High over the North Atlantic. Positive SLP anomalies of the Azores High and negative SLP anomalies of the Icelandic Low (Figs. 4C and D) are displayed in springs in which nssMg^{2+} concentrations are high and vice versa. Other obvious features are that the SLP anomalies over the Arctic and the Aleutian regions are connected with variations of 20D nssMg^{2+} records.

Fig. 5 reveals that Mt. Logan nssMg^{2+} records are related to the SLP of the Aleutian Low over the North Pacific. Springs in which nssMg^{2+} values are low/high (Figs. 5A and C) exhibit high/low anomalies for SLP of the Aleutian Low. The same pattern occurs for SLP over the East Arctic. Mt. Logan nssMg^{2+} has a connection with SLP anomalies over the Tibetan region in Asia and the Icelandic region over the North Atlantic (Fig. 5D).

To explore temporal relationships suggested by SLP difference fields in Figs. 3–5 we found, within those regions identified by the high–low SLP fields, those grid cells whose SLP records are most strongly associated with nssMg^{2+} concentration series. The SLP series from the multiple 5×5 degree grid cells thus identified (blackened in Fig. 1) were average to provide seasonal SLP histories throughout the instrumental period for each region. Correlation relationships between nssMg^{2+} concentrations and these SLP series of atmospheric centers are analyzed and correlation coefficients which are significant above 97% ($P < 0.03$) are summarized in Table 2. The significance levels shown in Table 2 are based on Monte Carlo estimation using a red noise null-model having the same auto-correlation as the appropriate SLP series. The correlation coefficients contained in Table 2 display highly significant linear relationships between nssMg^{2+} series and their dominant SLP centers of action, in particular, for these 5-year running values. The temporal comparisons between nssMg^{2+} concentrations and these SLP series are shown in Figs. 6–8.

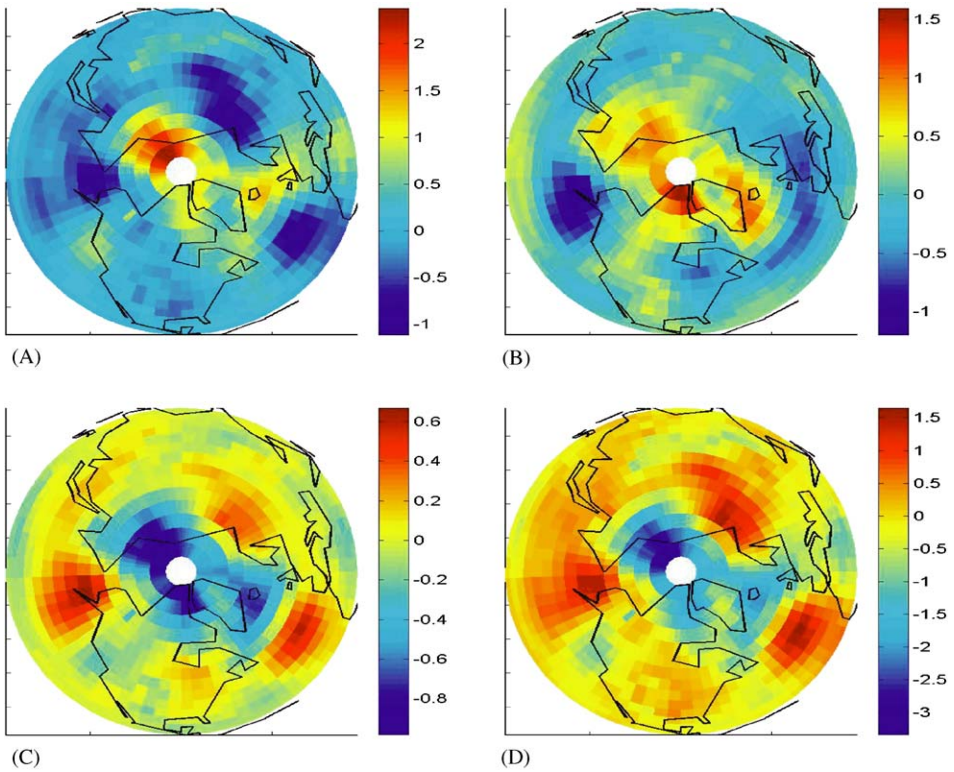

Fig. 4. Mean SLP field (all units: mb) calibrated with nssMg^{2+} concentrations from the 20D ice core: (A) mean SLP field anomaly in spring for the 29 years of lowest 20D nssMg^{2+} concentrations; (B) mean SLP field anomaly in spring for the 28 years of intermediate ones; (C) mean SLP field anomaly in spring for the 29 years of highest ones; and (D) difference SLP field in spring: mean anomaly of highest 29 years—mean anomaly of lowest 29 years.

4. Results and discussions

4.1. Dust aerosol transport over Asia

NssMg^{2+} in the Mt. Everest ice core is mainly correlated with the spring SLP series of the Tibetan High, the Arctic High, and the Azores High (Table 2 and Fig. 6). Positive relationships between nssMg^{2+} concentration and SLP of these Highs indicate that an enhanced Tibetan High, Arctic High and Azores High are favorable for dust aerosol transport from source regions to Mt. Everest. Spring is a transition season for atmospheric circulation over the Tibetan Plateau, when the Tibetan High gradually switches to the Tibetan Low (Bryson, 1986; Tang, 1998). An enhanced Tibetan High strengthens southward surface winds (Murakami, 1987) allowing more dust aerosols to be transported from desert regions over central Asia to the Himalayas, and a weakened Tibetan High corresponds to lower nssMg^{2+} values in the core. During the spring season, some of the dust storms over Asia are triggered by the cold front from the Arctic as they pass over desert regions (Qian et al., 1997). A stronger Arctic High may strengthen these cold front activities and cause stronger dust storms introducing more dust aerosols into the atmosphere. In the early spring, the southerly branch of the westerly jet remains positioned over the Himalayas (Barry and Chorley, 1998). A stronger Azores High strengthens eastward winds which potentially transport more dust aerosols from desert regions over south/west of Asia (e.g., Thar Desert), or even North Africa. It should be noted that nssMg^{2+} is more closely correlated with SLP changes of the Tibetan High than those of the Arctic High and the Azores High, especially for these 5-year running values (Table 2, Fig. 6), indicating that the influence of the Tibetan High is more important for dust aerosol transport to Mt. Everest than other two highs.

4.2. Dust aerosol transport to the south of Greenland

20D nssMg^{2+} concentrations are correlated positively with spring SLP series of the Azores High and the Siberian High, and negatively with these of the Icelandic Low and the Arctic High (Table 2 and Fig. 7). An enhancement of both the Siberian High and the Azores High corresponds to high nssMg^{2+} concentrations (e.g., 1900s and 1970s), while deepening of the Icelandic Low and weakening of the Arctic High are related to high

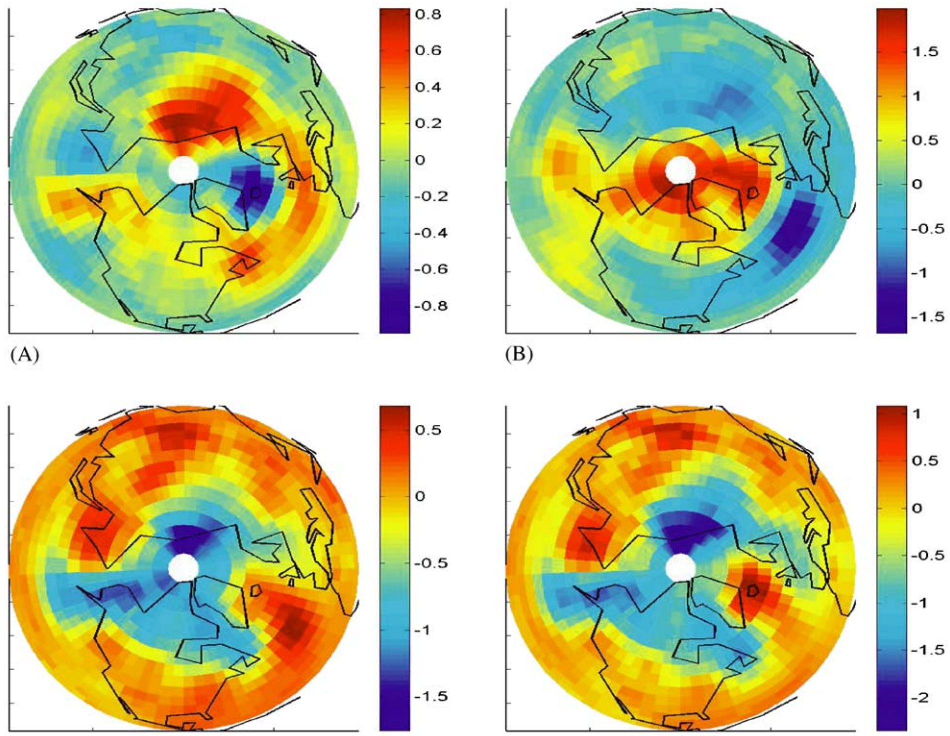

Fig. 5. Mean SLP field (all units: mb) calibrated with $nssMg^{2+}$ concentrations from the Mt. Logan ice core: (A) mean SLP field anomaly in spring for the 27 years of lowest Mt. Logan $nssMg^{2+}$ concentrations; (B) mean SLP field anomaly in spring for the 27 years of intermediate ones; (C) mean SLP field anomaly in spring for the 27 years of highest ones; and (D) difference SLP field in spring: mean anomaly of highest 27 years—mean anomaly of lowest 27 years.

Table 2
Correlations: $nssMg^{2+}$ concentrations from three ice cores and spring (March–April–May) SLP fields

Name	Latitude	Longitude	Number of cells	r (r')	P-value
Mt. Everest					
Tibetan High	35°N	90–105°E	2	0.24 (0.48)	<0.01
Arctic High	75–85°N	175°E–165°W	6	0.22 (0.39)	<0.03
Azores High	40–45°N	15–25°W	4	0.22 (0.25)	<0.03
20D					
Siberian High	50–60°N	40–70°E	5	0.23(0.43)	<0.03
Azores High	30–45°N	15–25°W	5	0.43 (0.57)	<0.00005
Icelandic Low	60–65°N	20–35°W	4	−0.23(−0.30)	<0.03
Arctic High	75–85°N	175°E–165°W	6	−0.36 (−0.54)	<0.0007
Mt. Logan					
Aleutian Low	55–70°N	170°E–165°W	6	−0.24	<0.03
Arctic High	70–85°N	40–120°E	8	−0.35 (−0.31)	<0.002
Tibetan High	30–35°N	75–100°E	5	0.26	<0.02

Note: r, correlation coefficient for annual value; r', for 5-year-running mean.

$nssMg^{2+}$ concentrations (Fig. 7). During the spring season, air mass trajectories reveal two transport pathways for air masses from Asia to Greenland (Kahl et al., 1997). One is a zonal transport route which passes subarctic region (the North Pacific and the North America) eastward to Greenland. The other is

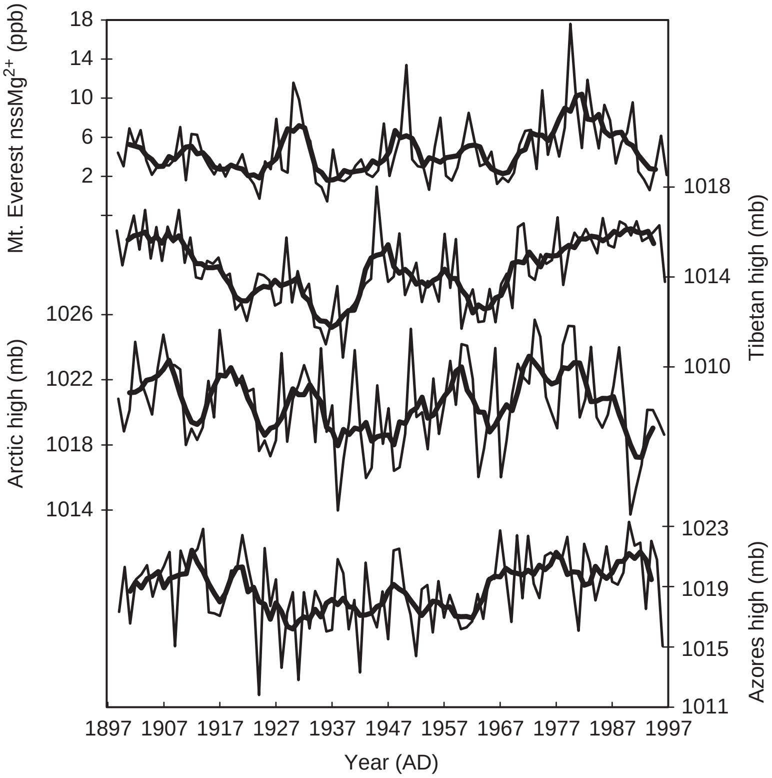

Fig. 6. Plots of the Mt. Everest annual nssMg^{2+} concentrations, spring SLP of the Tibetan High, the Arctic High, and the Azores High. The coarse lines are the 5-year running values.

meridional route which travels over the Arctic to Greenland. For both zonal and meridional routes, a stronger Siberian High, plus weakening of the Arctic High and deepening of the Icelandic Low are more favorable for dust aerosol transport from Asia to Greenland. Additionally, an enhanced Azores High and a deepening of the Icelandic Low, which can be described as a positive North Atlantic Oscillation (NAO) index phase, may strengthen meridional or zonal winds favoring dust transport to Greenland.

4.3. Dust aerosol transport to the Yukon Territory

NssMg^{2+} concentrations in the Mt. Logan ice core are correlated negatively with the spring SLP series of the Arctic High and the Aleutian Low, and positively with these of the Tibetan High (Table 2 and Fig. 8). Various studies have shown that every spring large quantities of mineral dust and pollution aerosols are carried eastward out of Asia and transported over a broad region of the North Pacific and North America (e.g., Gao et al., 1992; Arimoto et al., 1996; Prospero et al., 2003; McKendry et al., 2001). Both deepening of the Aleutian Low and enhancing of the Tibetan High, which are connected to high nssMg^{2+} concentrations, may strengthen the transport of air masses eastward bringing more dust aerosols from Asia to the Yukon Territory. A weakening of the Arctic High corresponding to high nssMg^{2+} values probably reflects that a feebler Arctic High may be favorable for the transport of air masses from Asia to subarctic regions and cause more dust deposition over the Yukon Territory.

4.4. Relationships between atmospheric circulations over the Northern Hemisphere

Since the teleconnections are a fundamental feature of the atmosphere, the changes in atmospheric circulations are not independent of each other. In order to explore the inter-SLP field relations over the Northern Hemisphere, we performed empirical orthogonal function (EOF) analysis on the six SLP time-series (Table 3). Here, multivariate EOF analysis is used rather than repeated simple linear regressions because EOF analysis allows a more robust assessment of the behavior of several variates and also provides new time-series that represent their relationships. EOF decomposition provides objective representations of multivariate data through the analysis of the covariance structure of its variates (e.g., Meeker et al., 1995). The EOF

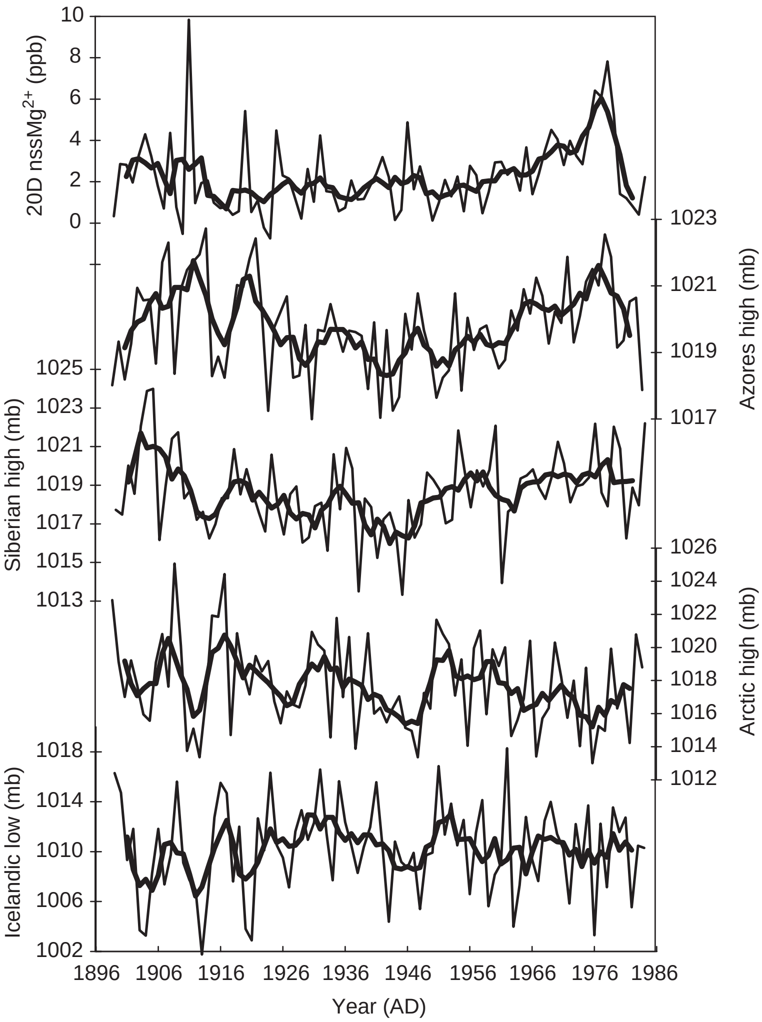

Fig. 7. Plots of the 20D annual $nssMg^{2+}$ concentrations, spring SLP of the Azores High, the Siberian High, the Arctic High, and the Icelandic Low. The coarse lines are the 5-year running values.

associations for the six SLP series in Table 3 demonstrate the correlations between atmospheric circulations. EOF1 accounts for 34.9% of the total variance in the six SLP series, and most of the Arctic High and Aleutian Low as well as partial Icelandic Low and Azores High (inverse relationship) are loaded on EOF1, indicating that the major SLP fields are close correlated with each other. Siberian High and Azores High dominate EOF2 and EOF4, suggesting a primary positive (EOF2) and a secondary negative (EOF4) correlation between two SLP fields. Tibetan High seems to be unique, which is strongly loaded on EOF3. The negative relationships between the Icelandic Low and Azores High are expressed in both EOF1 and EOF2, which can be described as NAO index as mentioned above. However, EOF5 also shows a minor positive correlation between two SLP fields. It is clear that changes in one SLP field almost inevitably impact most of the atmospheric system. It needs further studies on the mechanism of teleconnection processes.

It should be noted that a substantial part of the variability in the $nssMg^{2+}$ records cannot be explained by the changes in atmospheric circulation, although it has the statistically significant correlations with the identified SLP field anomalies. This implies that there might still be other factors influencing $nssMg^{2+}$ values. For example, precipitation variability might affect the removal of dust aerosols from the atmosphere by wet deposition. Atmospheric circulation is a complex process and any regional or local aspects of circulation could influence the snow chemistry in the glacier regions. These still need further more works to be demonstrated.

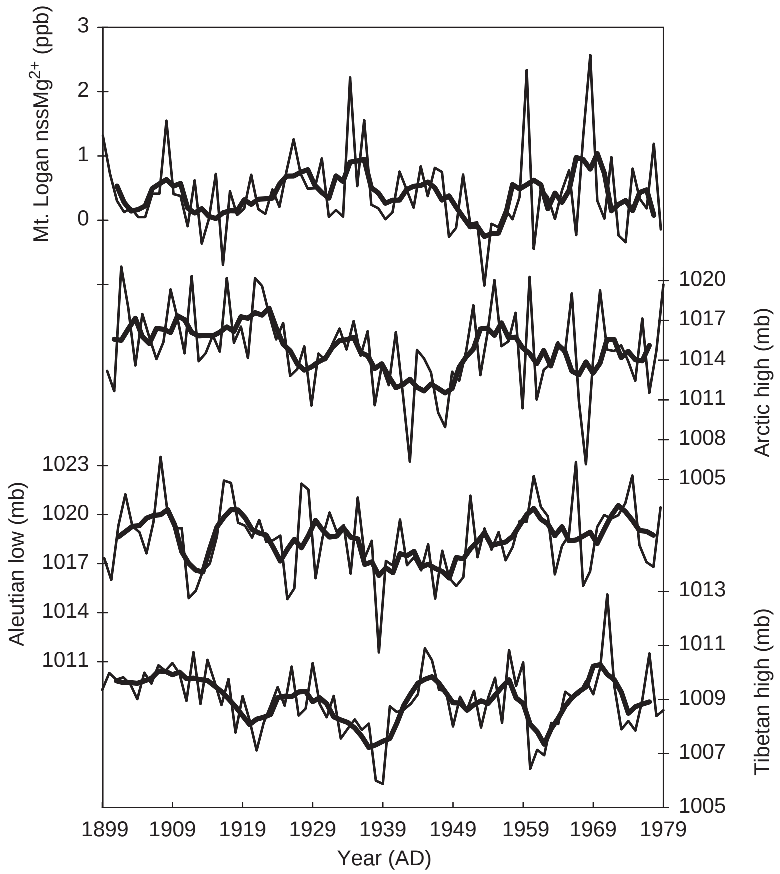

Fig. 8. Plots of the Mt. Logan annual $nssMg^{2+}$ concentrations, spring SLP of the Arctic High, the Aleutian Low, and the Tibetan High. The coarse lines are the 5-year running values.

Table 3
Results from empirical orthogonal function (EOF) analysis of spring SLP time-series over the Northern Hemisphere

	EOF1	EOF2	EOF3	EOF4	EOF5
Tibetan High	0.2	8.3	89.2	−0.1	−2.1
Azores High	−23.4	40.4	−0.2	−21.0	14.2
Siberian High	4.7	52.5	−0.7	39.2	2.8
Arctic High	75.1	5.9	0.0	−5.8	0.7
Icelandic Low	44.4	−25.9	4.4	0.2	22.1
Aleutian Low	61.5	11.0	−5.0	−5.0	−8.9
Total	34.9	24.1	16.6	11.9	8.5

Note: The numbers in the table represent the percent of variance associated with each SLP series. Negative values indicate an inverse relationship. Total numbers represent the percent of total variance in the SLP series explained by each EOF.

5. Summary and conclusions

Since the arid and semi-arid regions of central Asia are a major source area for dust aerosols over the Northern Hemisphere (e.g., Gao et al., 1992) and the peak in dust storm activity throughout central Asia occurs from mid-February to late May, with a strong maximum in late April–early May (Merrill et al., 1989), we concentrate on the relationships between non-sea-salt Mg^{2+}, an index of atmospheric dust from ice core records, from the Mt. Everest, the Mt. Logan, and the 20D ice cores and instrumental sea-level pressure (SLP) series of spring (March–April–May) in the last century (AD 1899–1996), in order to get insights into atmospheric transport patterns of spring dust aerosols over the Northern Hemisphere.

Mt. Everest $nssMg^{2+}$ concentrations are positively correlated with spring SLP of the Tibetan High, the Arctic High, and the Azores High. 20D $nssMg^{2+}$ records are positively correlated with the Siberian High and the Azores High SLP, while negatively correlated with the Arctic High and the Icelandic Low SLP in spring. Mt. Logan $nssMg^{2+}$ records have a negative relationship with SLP of the Aleutian Low and the Arctic High, and a positive relationship with the Tibetan High SLP in spring.

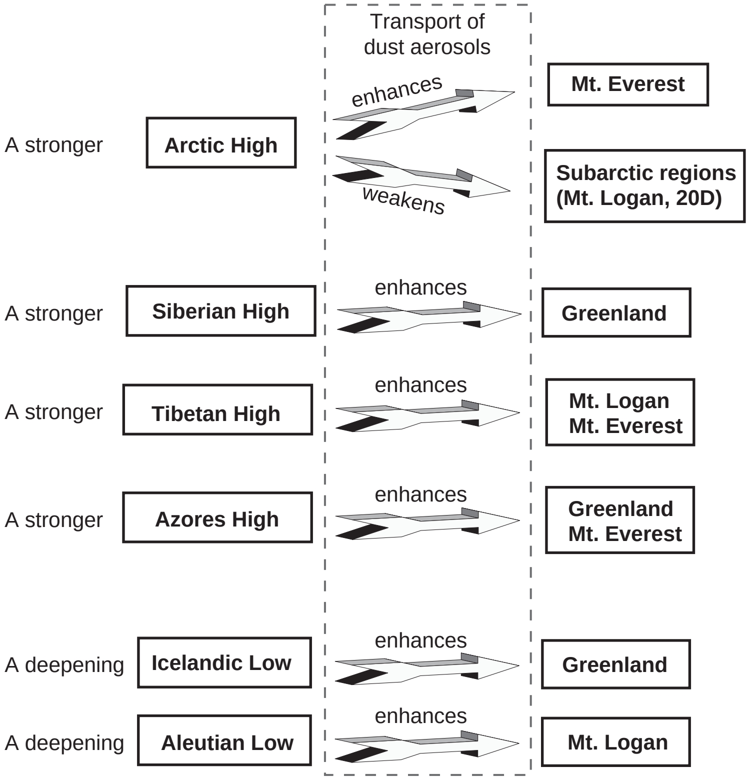

Fig. 9. Sketch of atmospheric transport patterns of spring dust aerosols over the Northern Hemisphere.

Based on the correlation relationships among $nssMg^{2+}$ series from the three ice cores and their positive and negative atmospheric centers of action, the spring dust aerosol transport patterns over the Northern Hemisphere are summarized in Fig. 9. On a hemispheric scale, an enhanced springtime Arctic High weakens dust aerosol transport from central Asia to subarctic regions (e.g., southern Greenland and Yukon Territory), but strengthens transport to the Himalayas (e.g., Mt. Everest). An enhancement of the Siberian High may strengthen transport of atmospheric dust to Greenland, and an intensification of the Tibetan High strengthens transport to the Himalayan and the Yukon regions in spring. A stronger spring Azores High favors dust transport to both the Himalayas and south Greenland. On a regional scale, a deepened springtime Icelandic Low and Aleutian Low increases transport of dust aerosols to Greenland and the Yukon Territory, respectively. It is becoming increasingly clear that teleconnections are a fundamental feature of the atmosphere, and the entire climate system. EOF analysis on SLP time-series indicates that changes in one region SLP almost invariably impact most of the system. It needs further studies on the mechanism of teleconnection processes. Understanding these transport patterns is significant for interpretation of ice core records and reconstruction of atmospheric circulation over the Northern Hemisphere using longer ice core records from these regions.

Acknowledgements

This research was supported by the US National Science Foundation (ATM 0139491); the Chinese Academy of Science (KZCX1-10-09/02; KZCX2-SW-118); the National Nature Science Foundation of China (Distinguished Innovation Group and G1999043401); Director Fund of Key Laboratory of Ice Core and Cold Regions Environment, CAS; the Electric Power Research Institute, the US Environmental Protection Agency, and the Environment Canada. We wish to thank members of the 1998 Glaciological Expedition on Mt. Everest, the Arctic Institute of North America, and University of Calgary for assistance and support in the field, S. Whitlow, W. Sun, M. Spencer, and C. Buck for analyzing samples from the three cores. We also greatly appreciate suggestions from Prof. Brimblecombe and the referee for the improvement of our paper.

References

Arimoto, R., Duce, R.A., Savoie, D.L., Prospero, J.M., Talbot, R., Cullen, J.D., Tomza, U., Lewis, N.F., Ray, B.J., 1996. Relationships among aerosol constituents from Asia and the North Pacific during PEM-West A. Journal of Geophysical Research 101, 2011–2023.

Barry, R.G., Chorley, J.R., 1998. Tropical weather and climate. In: Atmosphere, Weather and Climate, 7th Edition. Routledge, New York, pp. 235–288.

Bryson, R.A., 1986. Airstream climatology of Asia. In: Proceedings of the International Symposium on the Qinghai–Xizang Plateau and Mountain Meteorology. American Meteorological Society, Boston, MA, pp. 604–617.

Davidson, C.I., et al., 1993. Chemical constituents in the air and snow at Dye 3, Greenland—I. Seasonal variations. Atmospheric Environment A 27 (17/18), 2709–2722.

Favorite, F., Dodimead, A.J., Nasu, K., 1976. Oceanography of the subarctic Pacific region, 1960–1971. In: International North Pacific Fisheries Commission Bulletin, Vol. 33, pp. 187.

Gao, Y., Arimoto, R., Zhou, M., Merrill, J., Duce, R.A., 1992. Relationships between the dust concentration over eastern Asian and the remote North Pacific. Journal of Geophysical Research 97, 9867–9872.

Holdsworth, G., Krouse, H.R., Nosal, M., Spencer, M.J., Mayewski, P.A., 1989. Analysis of a 290-Year Net Accumulation Time Series from Mt. Logan, Yukon, in Snow Cover and Glacier Variations, Vol. 183. IAHS Publication, Baltimore, MD, pp. 71–79.

Husar, R.B., et al., 2001. Asian dust events of April 1998. Journal of Geophysical Research 106 (D16), 18317–18330.

Iwasaka, Y., Minoura, H., Nagaya, K., 1983. The transport and spatial scale of Asian dust storm clouds: a case study of the dust storm event of April 1979. Tellus B 25, 189–196.

Kahl, J.D.W., Martinez, D.A., Kuhns, H., Davidson, C.I., Jaffrezo, J.-L., Harris, J.H., 1997. Air mass trajectories to Summit, Greenland: a 44-year climatology and some episodic events. Journal of Geophysical Research 102 (C12), 26861–26875.

Kang, S., Wake, C.P., Qin, D., Mayewski, P.A., Yao, T., 2000. Monsoon and dust signals recorded in Dasuopu Glacier, Tibetan Plateau. Journal of Glaciology 46 (153), 222–226.

Kang, S., Mayewski, P.A., Qin, D., Yan, Y., Hou, S., Zhang, D., Ren, J., Kreutz, K., 2002a. Glaciochemical records from a Mt. Everest ice core: relationship to atmospheric circulation over Asia. Atmospheric Environment 36 (21), 3351–3361.

Kang, S., Mayewski, P.A., Qin, D., Yan, Y., Zhang, D., Hou, S., Ren, J., 2002b. Twentieth century increase of atmospheric ammonia recorded in Mt. Everest ice core. Journal of Geophysical Research, 107 (D21), 4595 (doi:10.1029/2001JD001413).

Kreutz, K.J., Mayewski, P.A., Pittalwala, I.I., Meeker, L.D., Twickler, M.S., Whitlow, S., 2000. Sea level pressure variability in the Amundsen Sea region inferred from a west Antarctic glaciochemical record. Journal of Geophysical Research 105 (D3), 4047–4059.

Legrand, M., Mayewski, P.A., 1997. Glaciochemistry of polar ice cores: a review. Reviews of Geophysics 35, 143–219.

Li, X., Maring, H., Savoie, D., Voss, K., Prospero, J.M., 1996. Dominance of mineral dust in aerosol light-scattering in the North Atlantic trade winds. Nature 380, 416–419.

Mayewski, P.A., Lyons, W.B., Spencer, M.J., Twickler, M.S., Koci, B., Dansgaard, W., Davidson, C., Honrath, R., 1986. Sulfate and nitrate concentrations from a South Greenland ice core. Science 232, 975–977.

Mayewski, P.A., Holdsworth, G., Spencer, M.J., Whitlow, S., Twickler, M.S., Morrison, M.C., Ferland, K.F., Meeker, L.D., 1993. Ice core sulfate from three Northern Hemisphere sites: source and temperature forcing implications. Atmospheric Environment A 27 (17/18), 2915–2919.

McKendry, I.G., Hacker, J.P., Stull, R., Sakiyama, S., Mignacca, D., Reid, K., 2001. Long-range transport of Asian dust to the lower Fraser Valley, British Columbia, Canada. Journal of Geophysical Research 106 (D16), 18361–18370.

Merrill, J.T., Uematsu, M., Bleck, R., 1989. Meteorological analysis of long range transport of mineral aerosol over the North Pacific. Journal of Geophysical Research 94, 8584–8598.

Meeker, L.D., Mayewski, P.A., 2002. A 1400 year long record of atmospheric circulation over the North Atlantic and Asia. The Holocene 12 (3), 257–266.

Meeker, L.D., Mayewski, P.A., Bloomfield, P., 1995. A new approach to glaciochemical time series analysis. In: Delmas, R.J. (Ed.), Ice Core studies of Biogeochemical Cycles, NATO ASI Series, Vol. 130. Springer, Berlin, pp. 383–400.

Moulin, C., Lambert, C.E., Dulac, F., Dayan, U., 1997. Control of atmospheric export of dust from North Africa by the Northern Atlantic Oscillation. Nature 387, 691–694.

Murakami, T., 1987. Effect of the Tibetan Plateau. In: Chang, C.P., Krishnamurti, T.N. (Eds.), Monsoon Meteorology. Oxford University Press, New York, pp. 235–270.

Overland, J.E., Heister, T.R., 1980. Development of a synoptic climatology for the northeast Gulf of the Alaska. Journal of Applied Meteorology 19, 1–14.

Parrington, J.R., Zoller, W.H., Aras, N.K., 1983. Asian dust: seasonal transport to the Hawaiian Islands. Science 220, 195–197.

Prospero, J.M., Savoie, D.L., Arimoto, R., 2003. Long-term record of nss-sulfate and nitrate in aerosols on Midway Island, 1981–2000: evidence of increased (now decreasing?) anthropogenic emissions from Asia. Journal of Geophysical Research, 108 (D1), 4019 (doi:10.1029/2001JD001524).

Qian, Z., He, H., Huo, Z., 1997. The classification and statistical characteristics of samples of dust storms in northwestern China. In: Fang, Z. (Ed.), Research of Dust Storm in China. Meteorological Press, Beijing, pp. 1–10 (In Chinese).

Qin, D., Hou, S., Zhang, D., Ren, J., Kang, S., Mayewski, P.A., Wake, C.P., 2002. Preliminary results from the chemical records of an 80 m ice core recovered from the East Rongbuk Glacier, Mt. Qomolangma (Everest). Annals of Glaciology 35, 153–158.

Sassen, K., 2002. Indirect climate forcing over the western US from Asian dust storms. Geophysical Research Letter 29 (10), 10.1029/2001GL014051.

Takemura, T., Okamoto, H., Maruyama, Y., Numaguti, A., Higurashi, A., Nakajima, T., 2000. Global three-dimensional simulation of aerosol optical thickness distribution of various origins. Journal of Geophysical Research 105 (D14), 17853–17873.

Tang, M., 1998. Formation, evolution and variability characteristics of Qinghai–Tibetan Plateau Monsoon. In: Tang, M., Chen, G., Lin, Z. (Eds.), Contemporary Climatic Variations over Qinghai–Tibetan Plateau and their Influences on Environments. Guangdong Sciences &Technology Press, Guangzhou, pp. 161–182.

Trenberth, K.E., Paolino Jr., D.A., 1980. The Northern Hemisphere sea level pressure data set: trends, errors and discontinuities. Monthly Weather Review 108, 855–872.

Wilson, J.G., Overland, J.E., 1987. In: Hood, D.W., Zimmerman, S.T. (Eds.), Meteorology, in the Gulf of Alaska. US Department of Commerce and US Department of Interior, Washington, DC, pp. 31–54.